



NIRSpec Performance Report NPR-2013-009/ESA-JWST-RP-19658

Authors: Marco Sirianni
Date of Issue: 24 May 2013
Revision: 1

Status of the NIRSpec Focal Plane Array # 104 after the second (FM2) cyro campaign.

Abstract:

The Focal Plane Assembly 104 was installed in NIRSpec during the second flight module cryo campaign (FM2) at instrument level held between December 2012 and February 2013 at IABG in Germany. This report summarizes the performance of FPA104 during FM2 and compares it with those observed during the first cryo campaign (FM1) carried out between January and March 2011.

1 INTRODUCTION

The detector system (DS) installed in NIRSpec during the first two Flight Module (FM) cryo campaigns (FM1 and FM2)¹ will also be used during ISIM cryo test #2 (CV2). It employs the Focal Plane Assembly (FPA) 104 with two Sensor Chip Assemblies (SCAs), two SIDECAR ASICs and the flight model Focal Plane Electronics (FPE). Table 1 lists the serial number of SCAs and ASICs installed in NIRSpec. The two SCAs have been classified as not flight worthy due to the on going degradation (addressed in section 5.2) and will be replaced after ISIM CV2. A different pair of ASICs, used to characterize the new FPA, will also be installed in such occasion.

Table 1. SCAs and ASICs installed in NIRSpec during FM2

Channel	SCA S/N	ASIC S/N
491	055	202
495	054	215

¹ FM1 occurred between Jan 2011 and March 2011, FM2 between December 2012 and February 2013.

This document summarizes the performance of the DS as measured with FM2 data and should be used as baseline for comparison with future data acquired during ISIM CV2 data. Additional information on the cosmetic of FPA104 is presented elsewhere [1].

All figures in this document, unless indicated otherwise, show images in the standard SCA orientation, as a normal FITS viewer would show them.

The structure of this document is as follow. In section 2 we verify the gain conversion coefficient used throughout the rest of this report. The superbias analysis is presented in section 3 while total noise is addressed in section 4. In section 5 we present the results of the analysis of dark exposures and the evolution of the number of hot pixels. In section 6 we summarize the performance of FPA104.

2 CONVERSION GAIN

The conversion gain and the relative pixel gain maps used in the pre-processing pipeline have been derived from data acquired at NASA/DCL [2]. Once the FPA is installed in NIRSpec it is no longer possible to illuminate simultaneously all the pixels of the FPA with a uniform signal level, and it is therefore impossible to measure and verify the gain at pixel level. We can only rely on the classical photon transfer curve method to determine the gain from regions with fairly uniform illumination level. Table 2 lists the exposures used to measure the gain during the preparatory phase of FM2 and to verify whether the DS was in need of additional “tuning”.

Table 2. Log of the exposures used to measure the conversion gain.²

NID	OBS_ID	4 4 F			FWA	GWA	CLS	CAA	MSA	DATE
		9 9 R	n n	n n						
		1 2 M	GRP	FRM INT						
7905	PREP-DET-CHECK-2-002	x x F	88	1	1	OPAQUE	G235H	CLOSE	FLAT5	SLIT5-A 2013-01-10
7906	PREP-DET-CHECK-2-003	x x F	88	1	1	OPAQUE	G235H	CLOSE	FLAT5	SLIT5-A 2013-01-10
7907	PREP-DET-CHECK-2-004	x x F	88	1	1	OPAQUE	G235H	CLOSE	FLAT5	SLIT5-A 2013-01-10

The images were processed following the procedure indicated in [3] and the classical photon transfer test was performed in two regions covering at least 4×10^4 pixels using the first ten groups of each ramp (Figure 1).

² NID= NIRSpec exposure unique identifier; OBS_ID= observation identifier; an X under 491 and 492 indicates that both SCA were operating, FMR=F indicate full frame exposures, n GRP, n FRM and n INT indicate respectively the number of groups, the number of frames in each group and the number of integration in a given exposure; FWA= configuration of the filter wheel assembly; GWA=configuration of the grating wheel assembly; CLS=configuration of the OGSE CLS; CAA=configuration of the CAA, MSA=uploaded MSA configuration file; DATE=date of the exposure.

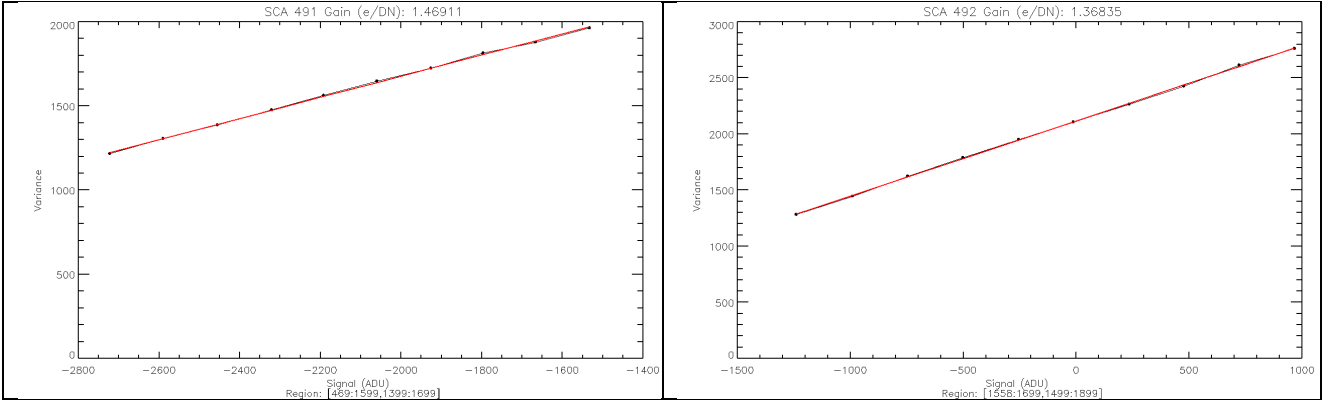


Figure 1. Classical photon transfer curve and conversion gain determination for pixels in a selected region of SCA 055 [491] (left) and SCA 054 [492] (right) during FM2.

The resulting gain conversion coefficients including the values corrected for intra-pixel capacitance are listed in Table 3. The agreement with the mean gain derived from data acquired at DCL is within a few percent.

Table 3. Conversion gain from FM2 data for FPA 104

SCA	Region	Gain e-/ADU	IPC corrected Gain e-/ADU	Ref. Gain (DCL) e-/ADU
S055 [491]	[469:1599,1399:1699]	1.590	1.469	1.453
S054 [492]	[1588:1699,1499:1899]	1.492	1.368	1.339

3 SUPERBIAS

Systematic pixel-to-pixel offsets and large scale gradients in the reset level are subtracted by the pre-processing pipeline [4] using a “master bias” or superbias obtained combining many first group images [5]. In addition to the first group of the standard dark exposures (each obtained as a single integration [Nint=1] of 88 groups [Ngroup=88]), dedicated exposures with Ngroup=1 and Nint=100 were acquired to build a high signal-to-noise superbias. Table 4 lists the dark exposures used to derive the superbias frame, dark current maps and total noise maps.

Table 4. List of dark exposures used to calculate total noise, superbias and dark current

Exposure Type	FM1			FM2		
	Exposure NID Range	Test Procedure	Date	Exposure NID Range	Test Procedure	Date
Ngroup=88 Nint=1	4536-4545	Prep-det-check-1	2011-02-05	8196-8225	Det-dark-short-1	2013-01-13
	6263-6275	Fill-det-dark-short	2011-02-28	10118-10137	Det-dark-short-2	2013-01-21
	6176-6292	Fiil-det-dark-short	2011-03-01	12231-12260	Det-dark-short-2	2013-01-30
				12261-12290	Det-dark-short-3	2013-01-30
Ngroup =1 Nint=100	4546	Prep-det-check-1	2011-02-05	8226	Det-dark-short-1	2013-01-13
				12291	Det-dark-short-3	2013-01-30

Figure 2 and Figure 3 compare the superbias frames (and the associated histogram for each output) derived from FM1 and FM2 data, respectively, for SCA055 [491] and SCA055 [492]. The overall systematic features and distribution of pixel-by-pixel reset level are remarkably similar between FM1 and FM2. There is one visible difference in the superbias frames between FM1 and FM2 for both SCAs. During FM1 a known issue with the ASIC microcode caused a lower offset level for the first two columns of each output resulting in a two-column wide dark line at the edges of the image and a four-column wide line at the centre. A newer ASIC microcode version used during FM2 resolved the issue.

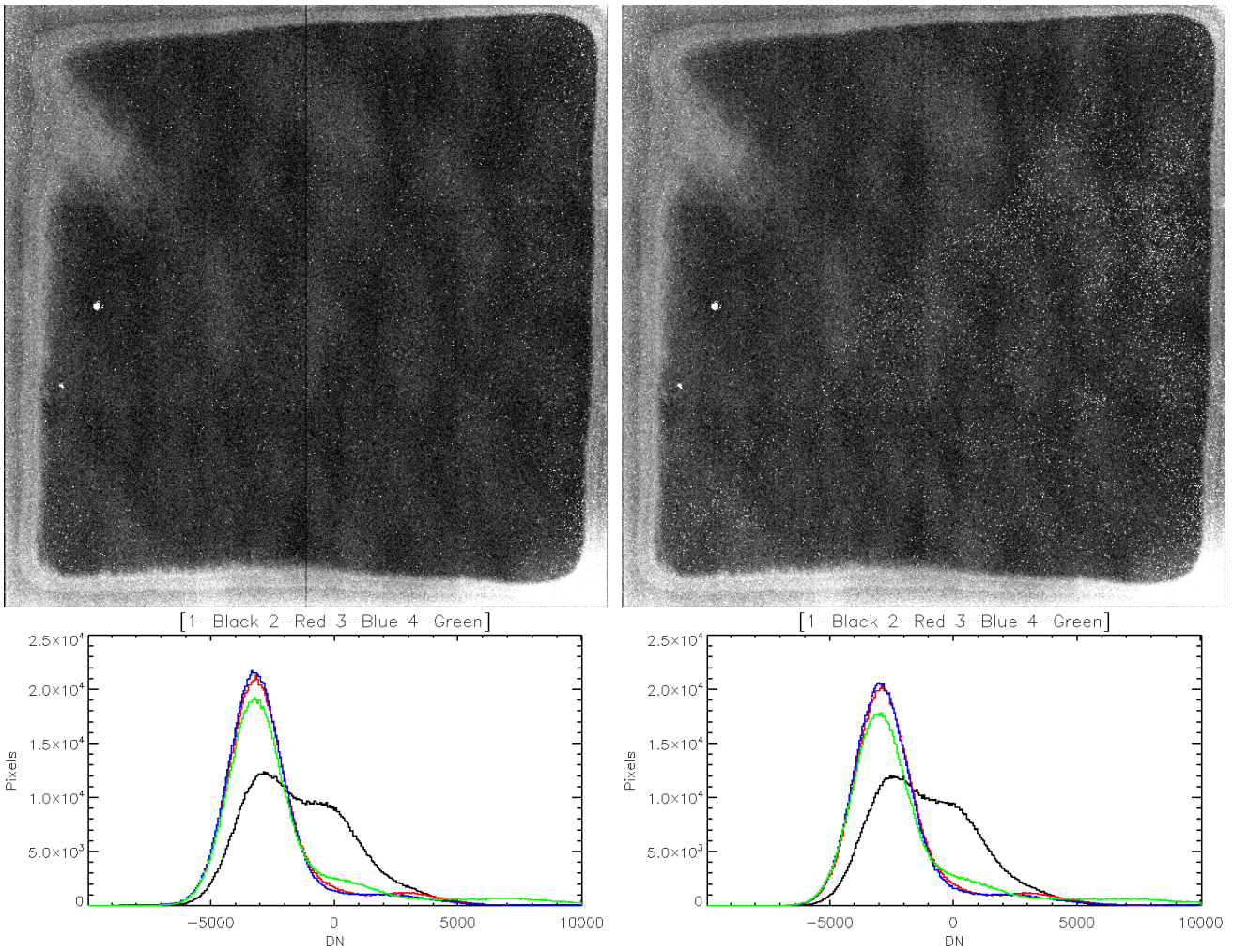


Figure 2. FPA104 SCA 055 [491] – superbias frames during FM1 (top-left) and FM2 (top-right). The two panels at the bottom show the relative histogram of the reset levels (after reference pixel correction) for each output [Output 1 – Black, 2- Red, 3- Blue, 4- green]

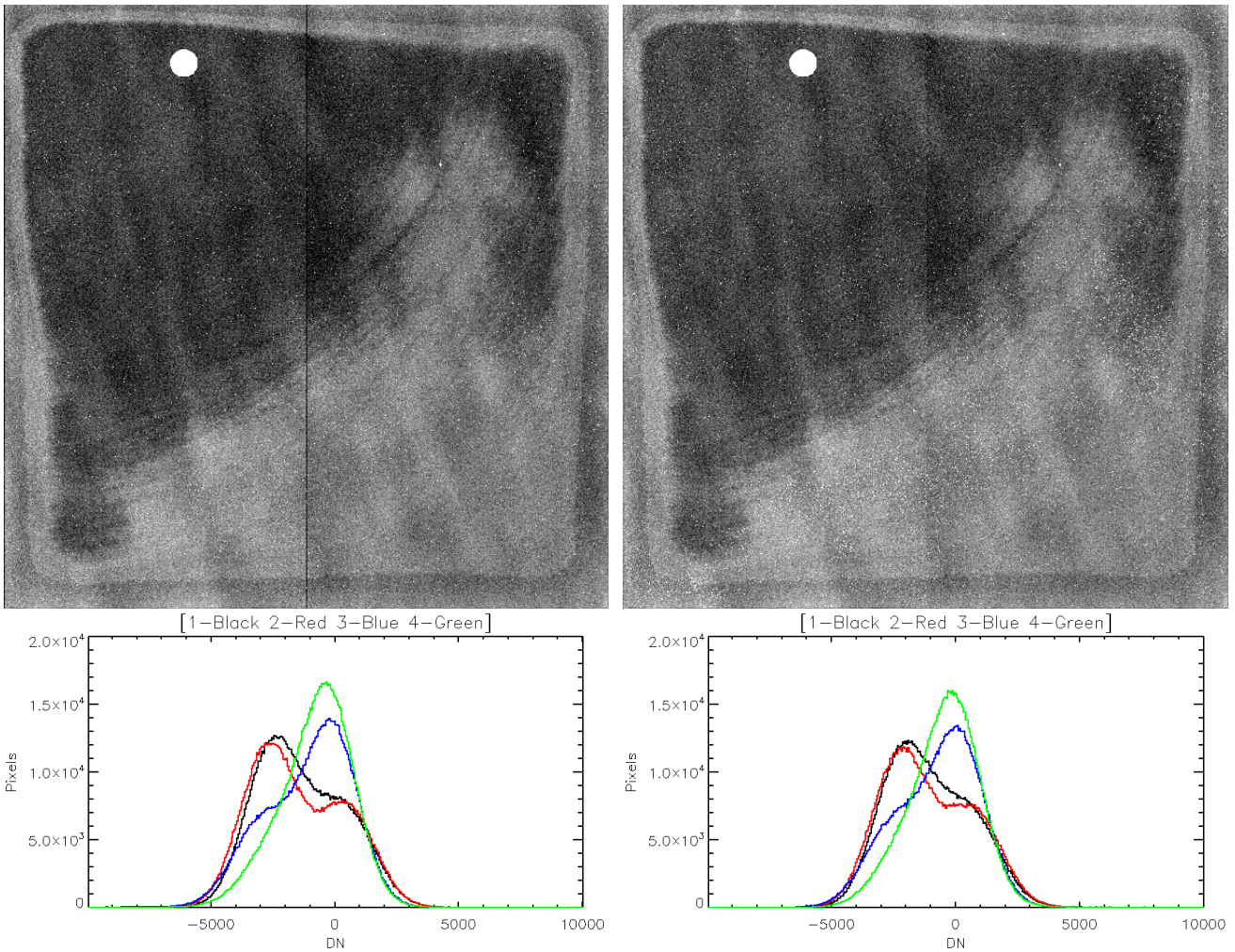


Figure 3. FPA104 SCA 054 [492] – superbias frame during FM1 (top-left) and FM2 (top-right). The two panels at the bottom show the relative histogram of the reset levels (after reference pixel correction) for each output [Output 1 – Black, 2- Red, 3- Blue, 4- green]

The histograms of the reset level distribution (after reference pixel level subtraction) shown in the bottom panels of Figure 2 and Figure 3 show very little variation between the two calibration campaigns. There is however a significant number of pixels that changed (becoming hot pixels as shown in section 5.1). This new population of hot pixels is clearly visible in the superbias image, in particular for SCA055 [491] (top right panel in Figure 2). A superbias frame is essentially a high S/N first read with frame time of 10.7 seconds and very hot pixels can accumulate a significant amount of charge in such time period. The histograms of the entire superbias frames (excluding reference pixels) are shown in logarithmic scale in Figure 4. The distributions show an increased number of pixels with high reset levels and therefore reduced dynamic range.

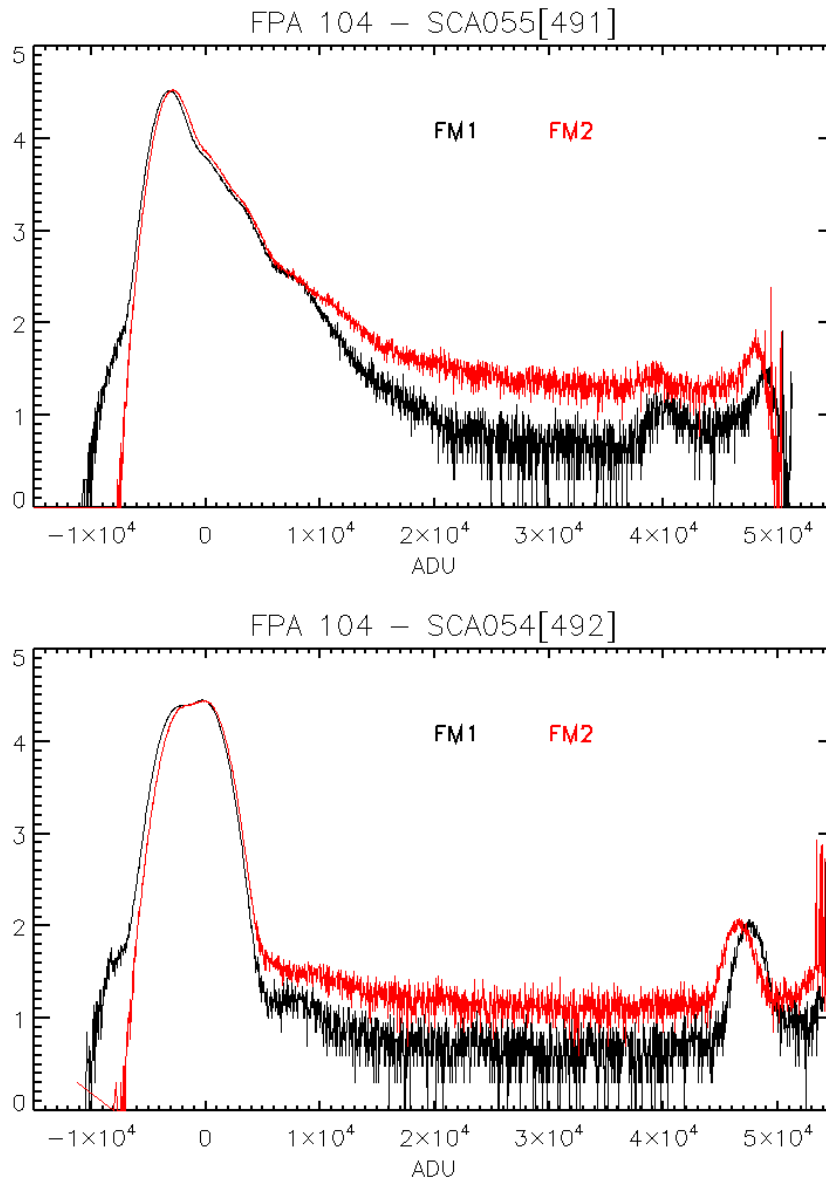


Figure 4. Comparison of the histogram of the superbias frames for SCA055[491] top and SCA054[492] bottom in logarithmic scale for FM1 and FM2

4 TOTAL NOISE

Total noise maps are created from the count rate images of all the dark exposures used to build the super-dark reference file [5] (using only the 88-groups exposures) listed in Table 4. For each pixel, the standard deviation over all the dark count rate images is computed after rejecting from the dataset the lowest and highest 5% of the distribution. The resulting standard deviation map is multiplied by the integration time of an 88-group exposure and by the gain map.

The noise maps (scaled between 3 and 15 e-) and the relative output-by-output histograms are shown in Figure 5 and Figure 6 for SCA055[491] and SCA054[492] respectively. The increased population of hot pixels is clearly visible in the total noise map created with FM2 data for both SCAs.

Table 5 and table 6 list the total noise measured in each output. For both SCAs the total noise measured during FM1 was in line with the DCL measurement [2], but increased on average by 10% to 17% in FM2 data for SCA 054[492] and SCA055[491], respectively. The same increase in noise is seen in active pixels and in reference pixels.

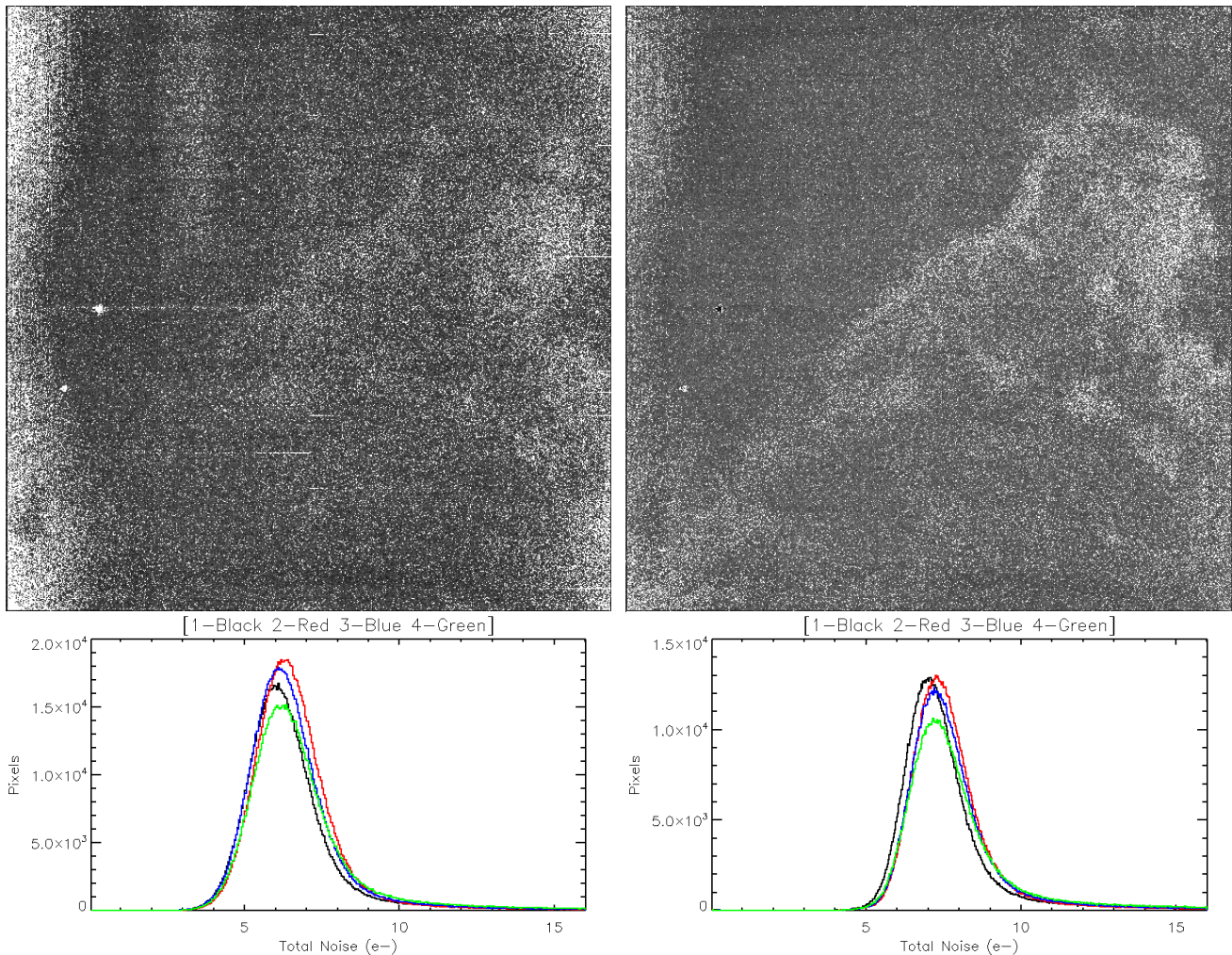


Figure 5. FPA104 SCA 055 [491] – Total Noise map during FM1 (top left) and FM2 (top right). The two panels at the bottom show the relative histogram of the total noise for each output [Output 1 – Black, 2- Red, 3- Blue, 4- green]

Table 5. Total Noise (e-) for FPA104 SCA055[491]

Region/Output	FM1				FM2			
	#1	#2	#3	#4	#1	#2	#3	#4
Top Ref Pixels	4.38	4.54	4.55	4.66	5.09	5.08	5.18	5.23
Active Pixels	6.02	6.43	6.30	6.61	7.24	7.49	7.48	7.57
Bottom Ref Pixels	4.39	4.42	4.48	4.54	5.04	5.01	5.09	5.11

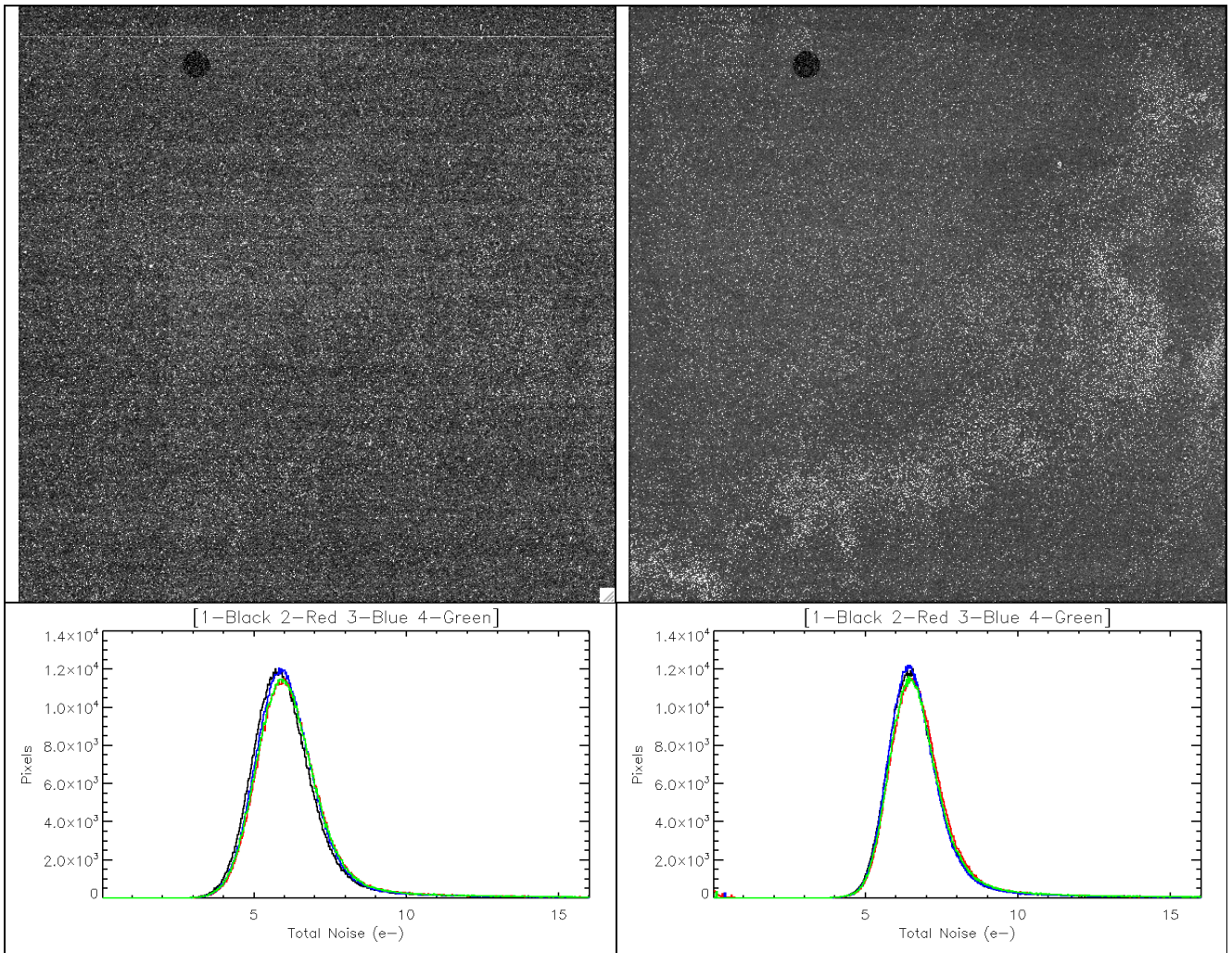


Figure 6. FPA104 SCA 054 [492] – Total Noise map during FM1 (top left) and FM2 (top right). The two panels at the bottom show the relative histogram of the total noise for each output [Output 1 – Black, 2- Red, 3- Blue, 4- green]

Table 6. Total Noise (e-) for FPA104 SCA054[492]

Region/Output	FM1				FM2			
	#1	#2	#3	#4	#1	#2	#3	#4
Top Ref Pixels	4.22	4.35	4.26	4.20	4.68	4.76	4.69	4.61
Active Pixels	5.94	6.09	6.03	6.08	6.59	6.68	6.58	6.65
Bottom Ref Pixels	4.26	4.38	4.37	4.32	4.70	4.83	4.76	4.72

5 DARK CURRENT AND HOT PIXELS

The same data used to measure the total noise (Table 4) were used to create the dark current cube reference file used by the pipeline [4]. From the dark cubes we can derive a 2D dark current map for the identification and flagging of hot and warm pixels. Figure 7 and Figure 8 show the dark maps and the relative histograms for SCA055[491] and SCA054[492], respectively, while Table 7 and Table 8 list the measured dark current in each output. Beside an overall increase of the number of hot pixels in both SCAs that will be addressed below, when compared with FM1 results the mean dark current for SCA055[491] shows an increase in particular for outputs #1 and #4. No appreciable difference is instead seen for SCA054[492].

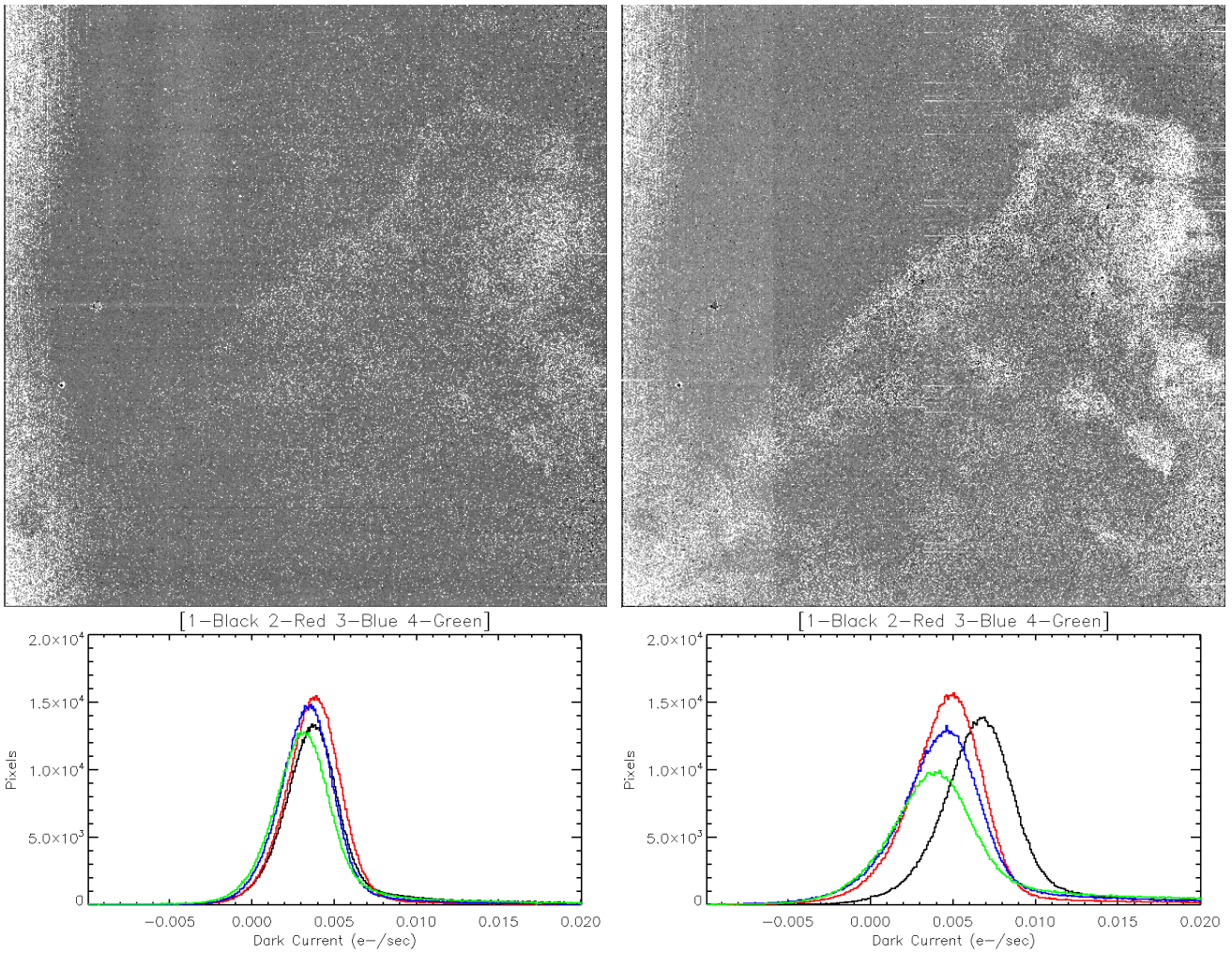


Figure 7 FPA104 SCA 055 [491] – Dark Current map during FM1 (top left) and FM2 (top right). The two panels at the bottom show the relative histogram of the dark current for each output [Output 1 – Black, 2- Red, 3- Blue, 4- green]

Table 7. Dark Current (e-/sec/pix) for FPA104 SCA055[491]

Region/Output	FM1				FM2			
	#1	#2	#3	#4	#1	#2	#3	#4
Mean	0.0037	0.0037	0.0033	0.0031	0.0066	0.0045	0.0043	0.0063
Stdev	0.0020	0.0019	0.0019	0.0021	0.0028	0.0029	0.0033	0.0041

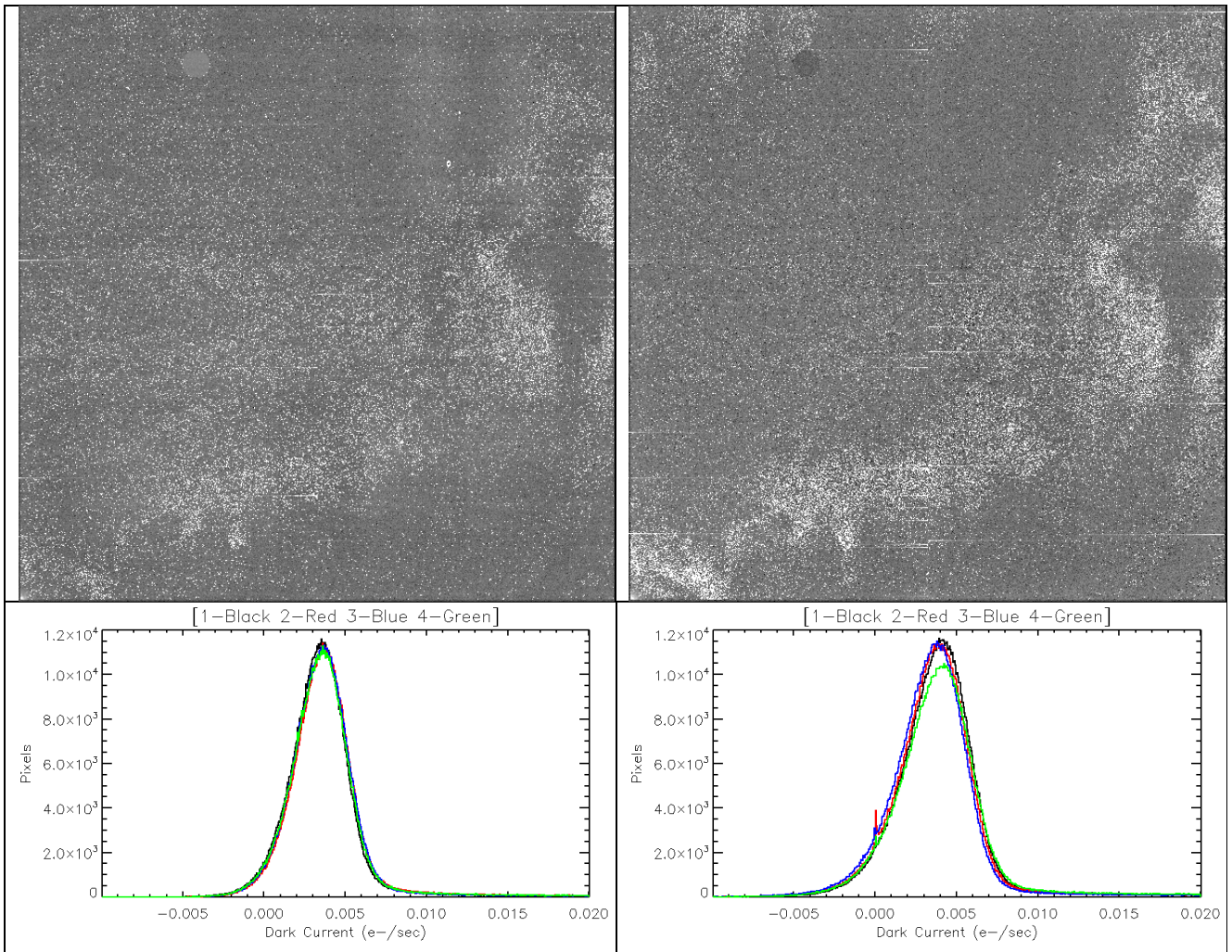


Figure 8. FPA104 SCA 054 [492] – Dark Current map during FM1 (top left) and FM2 (top right). The two panels at the bottom show the relative histogram of the dark current for each output [Output 1 – Black, 2- Red, 3- Blue, 4- green]

Table 8. Dark Current (e-/sec/pix) for FPA104 SCA052[492]

Region/Output	FM1				FM2			
	#1	#2	#3	#4	#1	#2	#3	#4
Mean	0.0033	0.0035	0.0035	0.0034	0.0037	0.0035	0.0033	0.0037
Stdev	0.0019	0.0019	0.0019	0.0020	0.0026	0.0026	0.0027	0.0027

5.1 Hot Pixels

The dark current distributions in the two SCAs of FPA104 shown in logarithmic scale in Figure 9 display an extended tail of pixels with elevated charge generation. Pixels with a dark current in excess of 0.1 e-/s are classified as “hot” and rejected by the pipeline. Pixels with dark current between 0.01 and 0.1 e-/s are classified as “warm” and are only flagged but normally processed by the pipeline.

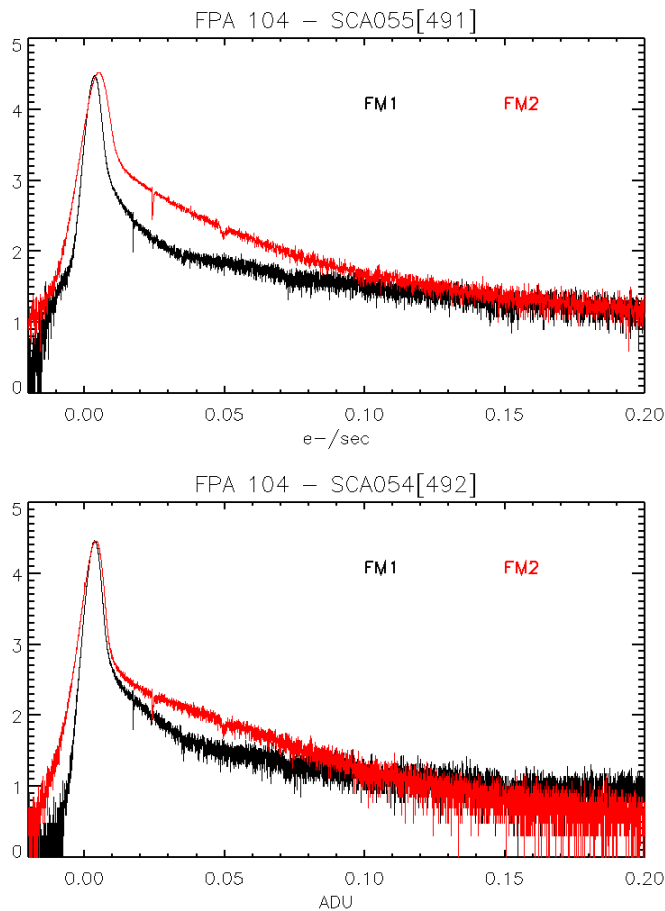


Figure 9. Histograms in logarithmic scale of the distribution of dark current for SCA055[491] (top) and SCA054[492] (bottom) for FM1 (black) and FM2 (red).

Due to intra-pixel capacitance (IPC), charge that is accumulated in one pixel is partly detected in neighboring pixels. To avoid to wrongly flagging a pixel as “hot” just because it neighbors a genuine hot pixels, the maps and statistics of hot pixels have been determined considering all pixels with dark current in excess to 0.1 e-/s after convolving the dark current ramps with an appropriate IPC kernel.

Figure 10 shows the distribution of hot pixels in the two SCAs of FPA104 during the FM2 cryo campaign. The number of hot pixels is very high in both SCAs reaching 3.3 % for SCA054 and 7.86% for S055.

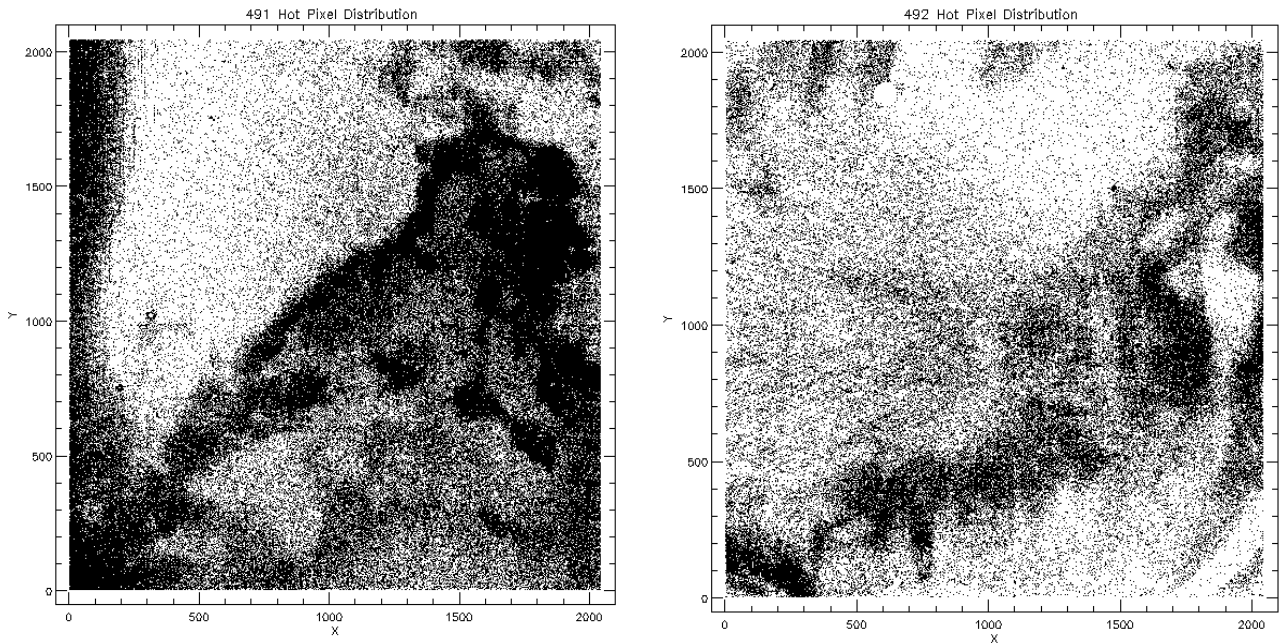


Figure 10. Hot Pixels [> 0.1 e-/sec] distributions for FPA104 during the cryo campaign FM2 at IABG in Jan-Feb 2013. SCA 055 [491] on the left and SCA 054 [492] on the right.

Table 9. Statistics of Hot and warm pixels in FM1 and FM2 data.

	FM1		FM2	
	SCA 055 [491]	SCA 054 [492]	SCA 055 [491]	SCA 054 [492]
Hot Pixels [> 0.1 e-/sec]	2.86 %	1.40 %	7.86 %	3.30 %
Warm Pixels [$0.01 < \text{e-/sec} < 0.1$]	7.18 %	3.55 %	13.32 %	6.21 %

5.2 EVOLUTION OF HOT PIXEL DEGRADATION

The two SCAs in FPA104 are among the first JWST 5.3 μm cutoff devices that showed degradation caused by a design flaw in the barrier layer of the pixel interconnect structure [6]. This degradation caused the FPA 104 to be classified as non-flight worthy.

Since FPA104 has been used in NIRSpec during the two cryo campaigns FM1 and FM2 we have an opportunity to address how the degradation has developed.

It should be noted that after FM1 the FPA104 had been returned to NASA to be held in cold storage at NASA/GSFC without further test or activities that would have changed or altered the FPA in any way. However in the period March-August 2012 the cold storage of FPA104 was interrupted several times due to power malfunctions [5]. As consequence the FPA104 went through six thermal cycles between ~ 60 K and ambient temperature before being re-delivered to Astrium.

Figure 11 shows the temporal evolution of the hot pixel distributions in the two SCAs in FPA104 from the initial testing at Teledyne in August 2008 to the last calibration campaign in February 2013. The hot pixel degradation has increased systematically over time (Figure 12). In particular, between FM1 and FM2 the number of hot pixel increased by a factor of 2.5. The number of “warm” pixels also doubled.

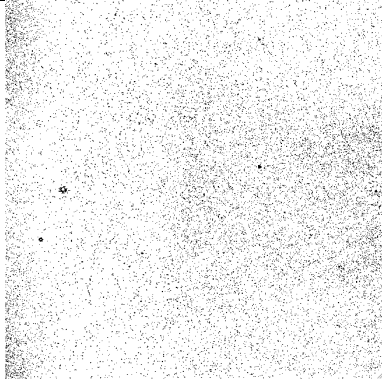
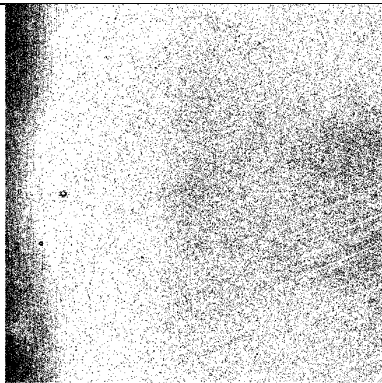
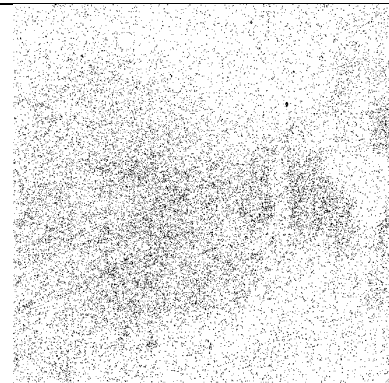
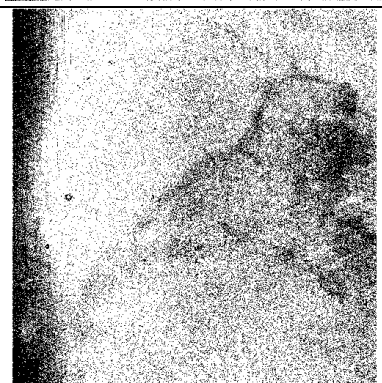
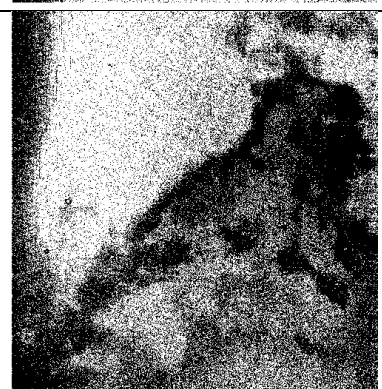
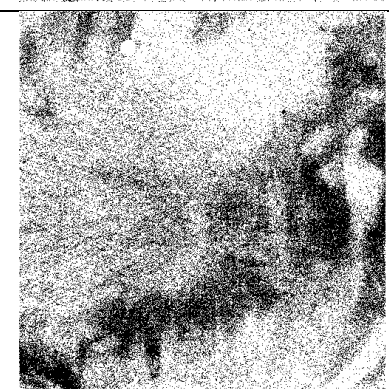
<p>Aug 2008 SCA 055</p> <p>Location: Teledyne Temp: 37K</p> <p>Percentage of Hot Pixels [> 0.1 e-/sec]</p> <p>0.95%</p>		<p>Aug 2008 SCA 054</p> <p>Location: Teledyne Temp: 37K</p> <p>Percentage of Hot Pixels [> 0.1 e-/sec]</p> <p>0.86%</p>	
<p>Jan 2010 SCA 055</p> <p>Location: DCL Temp: 38.5K</p> <p>Percentage of Hot Pixels [> 0.1 e-/sec]</p> <p>2.42 %</p>		<p>Jan 2010 SCA 054</p> <p>Location: DCL Temp: 38.5K</p> <p>Percentage of Hot Pixels [> 0.1 e-/sec]</p> <p>0.99%</p>	
<p>Feb 2011 SCA 055</p> <p>Location: IABG (FM1) Temp: 38.5K</p> <p>Percentage of Hot Pixels [> 0.1 e-/sec]</p> <p>3.55 %</p>		<p>Feb 2011 SCA 054</p> <p>Location: IABG (FM1) Temp: 38.5K</p> <p>Percentage of Hot Pixels [> 0.1 e-/sec]</p> <p>1.40 %</p>	
<p>Jan 2013 SCA 055</p> <p>Location: IABG (FM2) Temp: 38.5K</p> <p>Percentage of Hot Pixels [> 0.1 e-/sec]</p> <p>7.86 %</p>		<p>Jan 2013 SCA 054</p> <p>Location: IABG (FM2) Temp: 38.5K</p> <p>Percentage of Hot Pixels [> 0.1 e-/sec]</p> <p>3.30 %</p>	

Figure 11. Evolution of hot pixels degradation in SCA 055 [491] (left) and SCA 054 [492] (right)

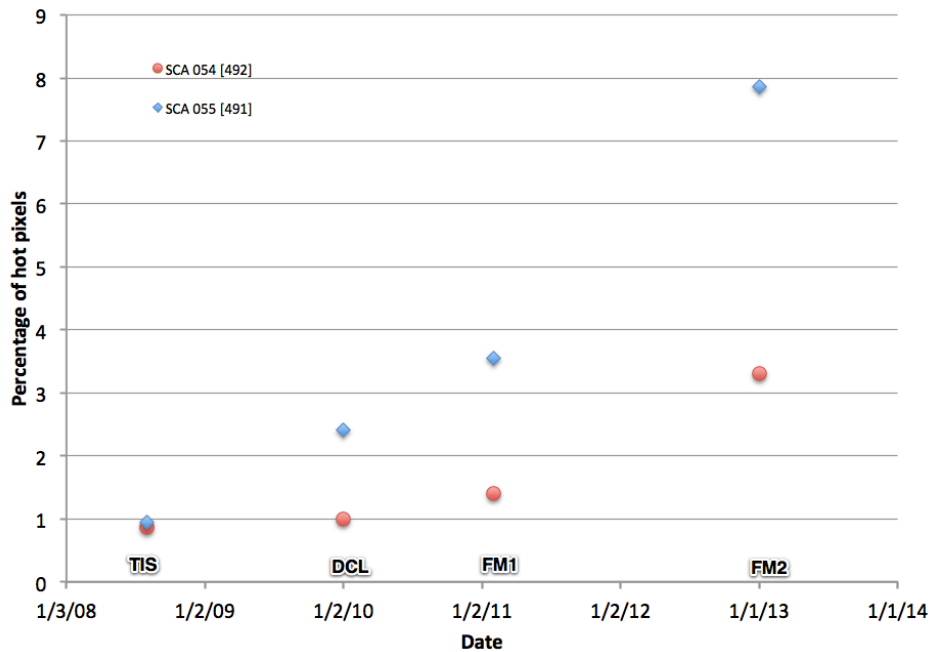


Figure 12. FPA104 Hot pixel contamination trend over a period of approximately 4.5 years

The high number of hot pixels and their distribution, in particular in SCA055[491], makes certain region of the FPA barely usable due to the very limited number of operable pixels. Figure 13 shows the hot pixel maps for the two SCAs in the “FPA orientation” with superimposed the approximate projection of the MSA quadrants.

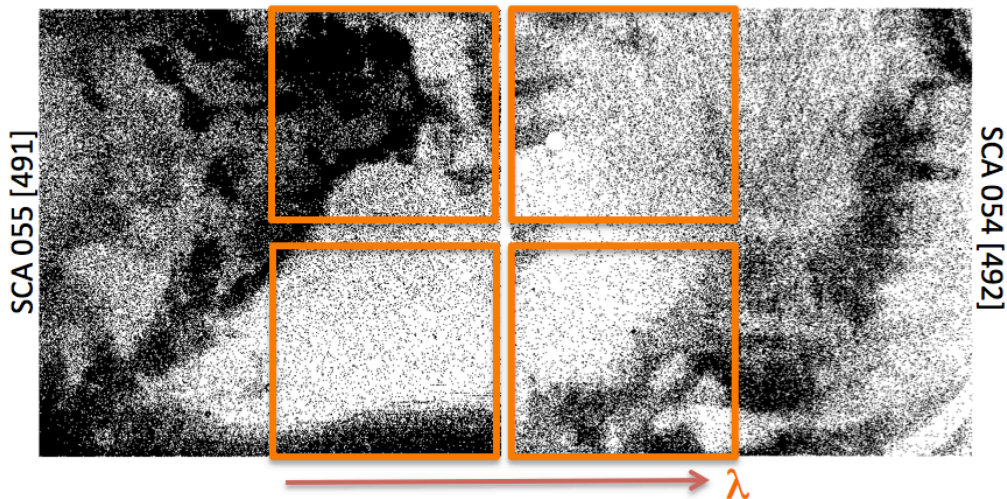


Figure 13. Hot pixel maps shown in the correct FPA orientation with over imposed the approximate projected layout of the four MSA quadrants.

6 SUMMARY

We have reviewed the high level performance of the two SCAs in FPA104 as measured during the cryo-campaign FM2 at IABG in early 2013. These are the main findings:

- Reset levels and gain conversion factors did not change compared to FM1 and they are in line with the original figures derived from DCL data.
- Compared to FM1 the total noise is increased by ~ 17% for SCA 055[491] and ~ 10% for SCA054[492]. Since the increase in total noise would have not compromised the quality of the calibration data acquired during the calibration campaign, a further optimization of the DS tuning was not deemed necessary.
- The mean dark current is slightly increased form SCA055[491] and it is unchanged for SCA054[492].
- The degradation of the two SCAs has continued despite the cold storage at NASA/GSFC at 60 K, which however was interrupted by 6 episodes of warming-up at ambient. The number of hot pixels has at least doubled since FM1.

7 REFERENCES

- [1]. NPR-2013-005/ESA-JWST-RP-19660 Average Responsive Quantum Efficiency and average distribution of bad pixels in NIRSpec SCAs – M. Sirianni <http://www.rssd.esa.int/lmlink/livmlink/open/3210442>
- [2]. JWST-RPT-016094 –Rev A- Near-Infrared Spectrograph (NIRSpec) Detector Subsystem (DS) Focal Plane Assembly S/N 104 Characterization Report
- [3]. NTN-2012-001 Prep-det-check: data analysis and result evaluation – M. Sirianni <http://www.rssd.esa.int/lmlink/livmlink/open/3209646>
- [4]. NTN-2011-004/ESA-JWST-TN-18257 Description of the NIRSpec pre-processing pipeline – S. Birkmann <http://www.rssd.esa.int/lmlink/livmlink/open/3100741>
- [5]. NTN-2011-005/ESA-JWST-TN-18258 NIRSpec Reference files and quality flags – G. Giardino et al. <http://www.rssd.esa.int/lmlink/livmlink/open/309938>
- [6]. JWST-RPT-017457 Detector Degradation Failure Review Board – root cause investigation <http://jwst.nasa.gov/resources/017457.pdf>
- [7]. JWST-EIDP-019969 - NIRSpec Detector Subsystem Focal Plane Assembly (FPA) FPA104 - Return Delivery End Item Data Package.